ФІЗИКА І ХІМІЯ ТВЕРДОГО ТІЛА
Т. 14, № 3 (2013) С. 566-571

PHYSICS AND CHEMISTRY OF SOLID STATE
V. 14, № 3 (2013) P. 566-571

PACS 81.05.UF: 72.80.-R: 05.60.GG

ISSN 1729-4428

M.P. Semen'ko, M.I. Zakharenko, T.V. Kalnysh

Transport Properties of the Graphite - Metal Nanocomposites

Department of Physics, Taras Shevchenko university, 64, Volodymyrska st.,
01601 Kyiv, Ukraine, e-mail: smp@univ.kiev.ua

The temperature behavior of the resistance of the thermo exfoliated graphite (TEG) and cobalt-containing nanocomposites on its base have been investigated. It is shown that the electrical properties of these materials could be easy explained within the incipient localization model. The influence of the metal modifier on the electric transport has been also analyzed.

Keywords: thermoexfoliated graphite, cobalt, electric resistance, weak localization; nanocomposite.

Стаття поступила до редакції 27.05.2013; прийнята до друку 15.06.2013.

Introduction

The potential applications of carbon based materials have caused a renewed interest in their development and investigation. In recent years there were several attempts to describe the electric transport of graphite and to deduce the temperature dependences of the resistivity [1-3]. Unfortunately all of them yield result only in special cases. Nevertheless, many of the graphite transport properties established during the last several years are being questioned at the present time. Conductivity measurements [2] reveal a suppression of the c-axis conductivity much larger than what would be predicted by the band structure calculations of the interlayer hopping. Band calculations are also challenged by recent observation of the quantum Hall plateaus in pure graphite [4, 5]

The analysis of electric properties in this case is strongly complicated by the presence of the high anisotropy of ρ for graphite crystal and peculiar conductivity mechanism in the disordered areas at the boundaries of the ordered graphite crystals. Especially high degree of disorder is inherent in TEG, so its electrical resistivity ρ is mainly governed both by its structure and morphology. That is why, the mechanisms determining the electric properties of the graphite-based structures remains still discussible.

Therefore, the purpose of our work was to consider the existing models of electric resistance and to select the most acceptable among them. So some speculations concerning the interpretation of ρ(*T*) dependencies for TEG are thoroughly analyzed in this paper. The same mechanisms have been involved in the analysis of resistivity of the TEG-based nanocomposites with cobalt and ascertaining a role of a metal component in formation of electric properties.

I. Experimental procedure

The specimens for investigation were prepared by the compacting of the source materials under the pressure ranging from 30 to 140 MPa. Table 1 shows the details of the specimens preparation. Specimens # 1 and # 2 were prepared of pure TEG, and # 3 and # 4 contained a cobalt component. Metal modifier has been involved into the structure of nanocomposite material by the routine chemical deposition.

The ρ(*T*) dependencies were investigated by the routine four-probe method within 77 - 450 K temperature range. In this case, the current was passed perpendicularly to the direction of pressing, i.e., along the direction of the dominant orientation of the graphite planes. The structure and morphology of the specimens have been controlled by the X-ray diffraction (Co-K_α radiation) and SEM (JEOL JCM-5000).

II. Experimental results

Fig. 1 shows the X-ray diffraction patterns of the investigated specimens. All diffraction spectra present sharp diffraction peaks of graphite. The presence of diffraction peaks of two orders allows to estimate the size of graphite particles *D* and the level of microstresses ε along the direction of pressing. Since the peaks were rather well described by the Lorentzian function, then the following expression was used to determine *D* and ε:

$$w\cos q / l = 1/D + 4e\sin q / l, \qquad (1)$$

where *w* is the width of the diffraction peak based on geometric broadening, θ is the position of the diffraction peak and λ is the X-ray wavelength.

Table 1

Characteristics of the investigated specimens

Specimen	Peculiarities	Preparation details	Heat treatment
#1	TEG	Routine procedure	–
#2	additional fragmented TEG	Impregnation by mineral-organic composition	T=800°C, τ=2 min
#3	TEG+CoO	Impregnation by aqueous solution of cobalt (II) nitrate; exsiccation	T=800°C, τ=2 min
#4	TEG+Co	Impregnation by aqueous solution of cobalt (II) nitrate; exsiccation; additional impregnation by mineral-organic composition	T=800°C, τ=2 min

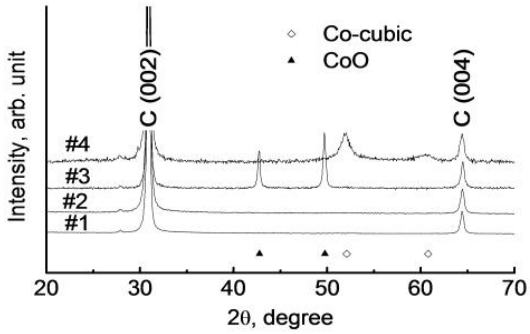

Fig. 1. X-ray diffraction patterns of the investigated specimens (numbering of the curves corresponds to the numbering, which is given in Table 1).

The obtained experimental results showed that $\varepsilon \sim 10^{-4}$ for all the specimens, i.e. it is possible to consider them to be quite negligible. At the same time, $D \sim 100$ nm for specimens #1 and #3, and $D \sim 50$ nm for specimens #2 and #4. The last two specimens have been additionally impregnated by a mineral-organic composition. These results demonstrate that the additional treatment by mineral-organic composition and subsequent heat treatment makes it possible not only to obtain the pure metallic component in the case of specimen # 4 (Fig. 1), but also provides the additional fragmentation of the TEG-particles. The heat treatment of TEG impregnated with the aqueous solution of cobalt (II) nitrate, leads to the formation of a cobalt (II) oxide (# 3, Fig. 1). The quite broad diffraction peaks (111) and (200) of *fcc*-cobalt were distinctly observed at the X-ray diffraction patterns for specimen #4. Since these maximums are formed by different types of planes, then it is not possible to use the Eq. (1) for determination of D and ε. Therefore, an estimation of the size D of cobalt particles has been performed by the Scherer's equation:

$$w = l / D\cos q \,. \qquad (2)$$

It was found that the size of cobalt particles is as high as 10 – 20 nm. The size of graphite crystallites and metal modifier particles allow to attribute these materials to nanocomposite.

The SEM-images of TEG particles surface of the investigated specimens were presented in Fig. 2. Comparing the images of the surfaces of # 1 and # 2 (pure TEG) specimens, one can be noted that the additional processing leads to the fragmentation of TEG particles. This is in consistence with the X-ray diffraction. In addition, a lot of bright irregularly shaped spots are visible on the particle surface. Obviously, these spots are the particles originated from the decomposition of mineral-organic component that was used for additional treatment. Its composition suggests that these particles consist of carbon. No other peaks except for graphite were detected in the X-ray spectra of these specimens , that confirms the above assumption.

The shape of the cobalt (II) oxide particles (specimen # 3) is almost spherical. Their size is about 100 nm. Treatment of the specimens with mineral-organic solution significantly modifies the distribution of particles over the surface of graphite (Fig. 2, d). Since the concentration of nitrate was the same (30 wt.%) for the specimens # 3 and # 4, then it is evident that the process of reduction with the mineral-organic composition leads not only to fragmentation, but also to a partial immersion of cobalt particles into the TEG.

Temperature dependencies of the normalized electrical resistance of the specimens are shown in Fig. 3. *R(T)* dependencies for TEG containing no metallic component are presented in Fig. 3, a. In this case, the specimens of TEG without any additional treatment were pressed at P = 30 MPa (# 1-1) and 140 MPa (# 1-2). All other specimens were compacted at P = 30 MPa. *R(T)* dependencies for the specimens with Co component are shown in Fig. 3, b. Although normalized dependencies R/R_{300} for different specimens are seen to be almost similar, (except for specimen # 2), but the absolute values of the electric resistivity ρ (at room temperature) are quite different. It is equal to 9 ± 1 μΩ×m and 6 ± 1 μΩ×m for specimens # 1-1 and # 1-2, 55 ± 5 μΩ×m for specimen # 2, 20 ± 2 and 61 ± μΩ×m 5 for # 3 and # 4 specimens, respectively.

III. Discussion

Decreasing *R(T)* dependence is typical for graphite

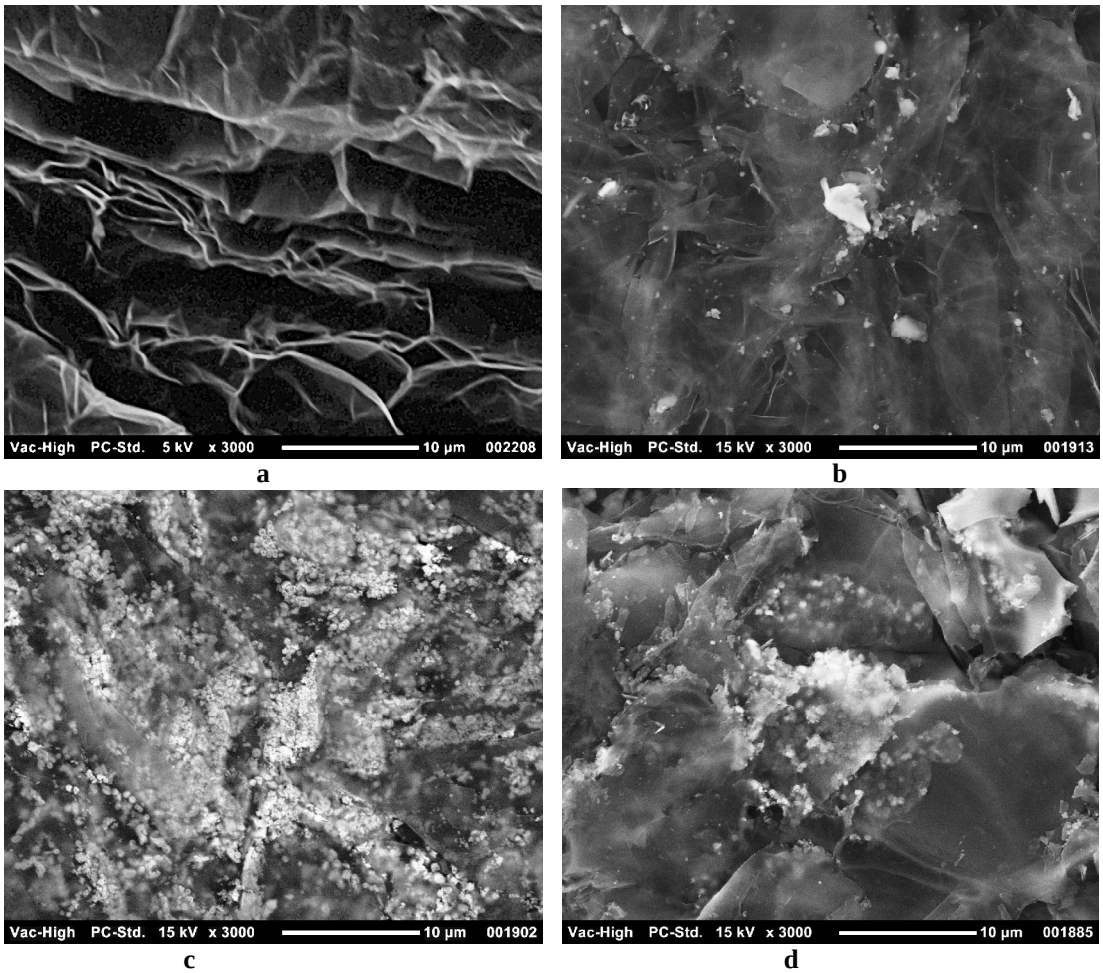

a **b**

c **d**

Fig. 2. The SEM-images of TEG particles surface of the investigated specimens: **a** - pure thermoexfoliated graphite (TEG) #1; **b** - additionally fragmentized TEG #2; **c** - TEG-CoO; **d** – TEG-Co.

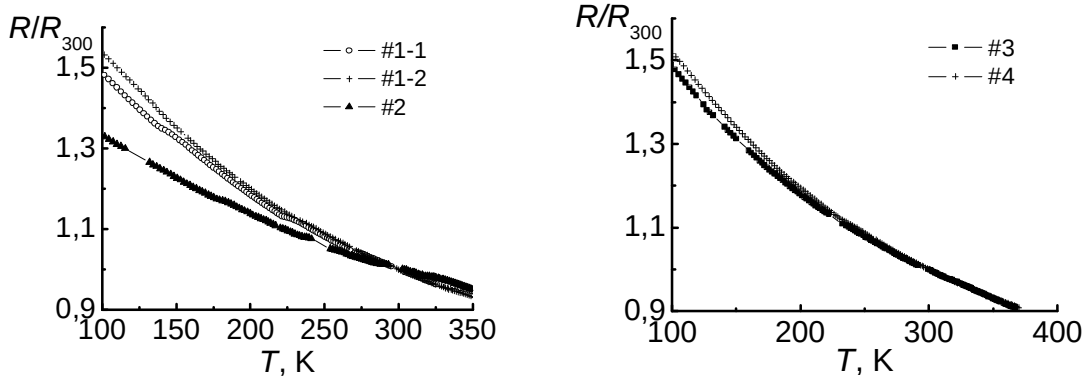

a **b**

Fig. 3. Temperature dependences of the normalized electrical resistance of the specimens.

specimens even when the current is passed along the preferred orientation of graphite planes. It demonstrates such a behavior as a result of the contribution to the electric resistance of the boundaries and disordered part of graphite. Investigation of *R(T)* at high temperatures (is not considered in this paper) shows a minimum for this dependency at *T* higher than 750 K. This fact suggests that this relationship is formed by two contributions: increasing, metal type, arising from the electric resistance along the hexagonal planes of crystalline graphite, and either increasing or decreasing contribution from the boundaries and disordered parts of graphite. Let's assume that the temperature dependence of the resistance of graphite along the basic plane could be described by the expression:

$$R_C = R_0 + \alpha T, \quad (3)$$

and the electric resistance due to disordered interparticle boundaries is of the activation character [3], i.e.:

$$R_A = R_m \exp(E_a/kT), \quad (4)$$

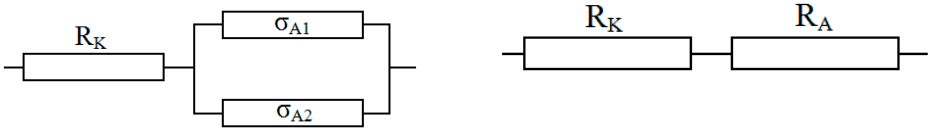

a **b**

Fig. 4. The equivalent circuits of used models of electrical resistance (Eq. 5 and 6)

where E_a is the activation energy, k is the Boltzmann constant, R_m is the pre-exponential factor.

In this case, according to the equivalent circuit shown in Fig. 4, a, the total electrical resistance could be expressed as:

$$R=R_C+R_A=R_0+\alpha T+R_m\exp(E_a/kT). \quad (5)$$

The fitting of the experimental data showed that they would be well described by a such type of function, but the negative values of E_a and R_m, was found by fitting. This fact gives the reasons to consider this model of resistance possessing no physical meaning.

However, the presence of the negative contribution to the activation energy and R_m can also occur within the further electric models. Its equivalent circuit is shown in Fig. 4, b. If we assume that the interfacial electric transport is realized due to two types of the charge carriers, then:

$$1/R_A = s_A = s_{A1} + s_{A2}, \quad (6)$$

where σ_A, σ_{A1} and σ_{A2} are respectively the total conductivities and conductivity due to two types of the carriers.

If $s_{A1} = s_{A01} = const$ (carriers with low activation energy) and $s_{A2} = s_{m2}\exp(-E_a/kT)$, then R_A could be expressed as:

$$R_A \approx 1/s_{A01} - R_m\exp(-E_a/kT), \quad (7)$$

if $\sigma_{A01} >> \sigma_{m2}\exp(-E_g/kT)$. Here, $R_m = \sigma_{m2}/(\sigma_{A01})^2$.

The results of fitting of the experimental curves according to Eq. (7) are presented in Table 2. The values of α were found to be less than 10^{-4} K^{-1} (both, either positive or negative) were obtained for different specimens. That is why α could be considered to be equal to zero within the accuracy of experiment. Although the values of E_a were found to be close to that obtained for graphite [3], the absence of a growing contribution can not explain the occurrence of the minimum of electrical resistance. This fact "this fact indicates that the model is wrong.

It is widely known that specific behavior of *R(T)* in disordered structures could be explained in terms of additional contributions to the resistivity due to the mechanisms of weak localization (WL) and electron-electron interaction (EEI) [6, 7]. EEI mechanism is significant only at relatively low *T* (extremely lower the temperature range of our study). At the same time, the mechanism of WL can provide an essential contribution to resistivity even at higher temperature. The mechanism of WL is also used to interpret the electric transport of graphite [8]. Nevertheless, the so-called model of incipient localization [6] was not used for this purpose. This model, in part, was shown to be successful in description of the features of the temperature behavior of the resistance for a series of amorphous alloys [9]. Since the studied composites contain a significant amount of disordered graphite, this model is thought to be worthwhile in explanation the temperature dependences *R(T)* of the investigated structures.

Table 2

The results of fitting of the experimental curves according to Eq. (7)

Specimen	R_0	R_M	E_a/k, K
#1-1	1,68	1,27	188
#1-2	1,74	1,37	188
#2	1,42	0,92	234

Within the model of incipient localization the conductivity could be expressed as:

$$s(T) = s_{B0} - s_B(\dot{O}) + \Delta s_{WL}(T), \quad (8)$$

where σ_{B0} is the temperature independent part of the Boltzmann conductivity, $\sigma_B(T)$ is its temperature dependence and $\Delta s_{WL}(T)$ is the contribution due to WL-effect:

$$\Delta s_{WL}(T) \cong \frac{1}{p^2}\frac{e^2}{\mathbf{h}}\frac{1}{L_i(T)}. \quad (9)$$

Here $L_i(T)$ is a diffusion length:

$$L_i(T)^2 = 1/2(l_e l_i), \quad (10)$$

l_e is an elastic scattering length and l_i is an inelastic scattering length.

The usability condition of the WL effects is $l_i >> l_e$ [7]. Elastic scattering length l_e in highly disordered structures is limited to the average interatomic distance and may be considered as temperature-independent parameter. The inelastic scattering length l_i is $\sim T^{-2}$ at $T<\Theta_D/3$ (the Debye temperature) and $\sim T^{-1}$ at $T>\Theta_D/3$ [6]. As a result, a temperature region where there is a contribution proportional to $T^{1/2}$ should be expected, that directly proceeds from Eq. (10).

If $\sigma_B(T)$, $\sigma_{\Delta WL}(T) << \sigma_{B0}$, then

$$r(T) = r_{\text{Á}0} + r_{\text{Á}}(\dot{O}) - \Delta s_{\text{ÑÈ}}(T)\cdot r_{\text{Á}0}^2 \quad (11)$$

Here, the Boltzmann resistivity is caused by metal-type conductivity in crystalline graphite, then the normalized electrical resistivity within a certain temperature range is

$$r(T) = a_0 + a_1\dot{O} - e_{1/2}T^{1/2} \quad (12)$$

The experimental curves were found to be fitted

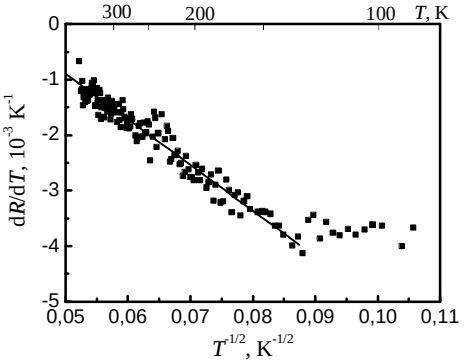

Fig. 5. Temperature dependence of the temperature derivative of the electrical resistance.

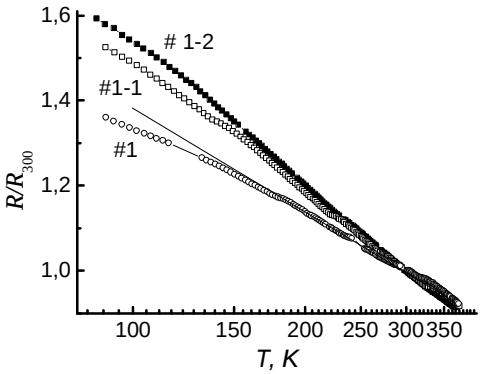

Fig. 6. Temperature dependences of electrical resistance in logarithmic scale.

quite well by the function (12). For a more convincing proof of the presence of the contribution proportional to $T^{1/2}$, we find the derivative *dr/dT*. Since $dr/dT = a_1 - 1/2 e_{1/2} T^{-1/2}$, the dependence, being plotted in *dR/dT vs.* $T^{1/2}$ coordinates, should exhibit a linear behavior.

Really, the curves, derived from the experimental data, exhibit such behavior within a certain temperature range (Fig. 5). The appropriate fitting parameters are given in Table 3.

Withal, $r(T) = r - e_{1/2} T^{1/2}$, then

$r(T) \approx r \ln r - 1/2 r \ln T - r \ln e_{1/2}$ if $r(T)/r << 1$

Therefore, the *R(T)* dependencies exhibit a linear region if they are plotted in logarithmic scale (Fig. 6).

In addition, the inelastic scattering length l_i is determined by the density of electronic states at the Fermi level $N(E_F)$: $l_i \sim 1/N(E_F)$ [10]. Since, according to calculations of the electronic structure of amorphous carbon, E_F is near the minimum of *N(E)* [11], so the high value of l_i should be expected.

Let's estimate the value of l_i using the values of ρ_{300} and fitting parameters listed in Table 3. Here, the value of l_e was taken to be equal to 0,3 nm and following equation was used:

$$e_{1/2} T^{1/2} = \frac{1}{p^2} \frac{e^2}{\mathbf{h}} \frac{1}{L_i(T)} \frac{r_{Á0}^2}{r_{300}} = \frac{1}{p^2} \frac{e^2}{\mathbf{h}} \frac{a_0^2 r_{300}}{L_i(T)} \quad (13)$$

The values of L_i and l_i at $T = 300$ K for the investigated materials are also presented in Table. 3. As seen from these data, a condition $l_i >> l_e$ is satisfied for all the specimens. In addition, the specimens which were additionally treated (# 2, # 4 and # 3) differ by a significantly increased value of l_i. This result is consistent with structural studies completely. This provides an additional evidence for the possibility of the adequate description of the transport properties of graphite structures using the mechanism of WL.

Table 3

The appropriate fitting parameters according to Eq. (12) and scattering characteristics of the conduction electrons

Specimen	ρ,μΩ·m	a_0	a_1, 10^{-3} K^{-1}	$\varepsilon_{½}$, $K^{-½}$	L_i (300K), nm	l_i (300K), nm
#1-1	9	2.81	3.10	0.16	0.6	2.7
#1-2	6	2.69	2.46	0.14	0.4	1.3
#2	55	1.97	0.88	0.07	4.4	126
#3	20	2.71	2.64	0.14	1.5	15
#4	61	2.55	2.25	0.13	4.4	126

The influence of cobalt on the electrical resistance can be also analyzed using the described approach. The data presented in Table 3 show that specimens # 2 and # 4, which had the same thermochemical processing, exhibit extremely high ρ values. Although the fitting parameters of their normalized dependencies *R(T)* are different, the inelastic scattering length l_i is almost the same. This suggests that the electric transport (at least in a case of *dc* measurement) of TEG-cobalt nanocomposites is formed by the graphite matrix predominantly, and the role of metallic cobalt particles is insignificant. This may be conditioned by the formation of oxides or carbides at the surface of cobalt nanoparticles. These "skins" almost totally isolate them from the graphite matrix. Partial confirmation of this fact may be deduced from the results obtained for specimen # 3, which containing nonconductive particles of a cobalt (II) oxide. Obviously, this increasing of the resistivity for this nanocomposite material is caused not only by the additional disordering of graphite matrix, but also by the reducing of the effective cross section due to nonconductive particles.

Conclusions

Thus, the paper shows that the incipient localization model could satisfactorily describe the electrical properties of graphite structures. Basing on this model we can say that the role of the metallic component in the *dc* conductivity, at least in nanocomposite materials, which were synthesized by the proposed method, is

negligible. This may be due to the formation of the insulating layer on the surface of nanoparticles.

Acknowledgement. This work was partially supported by the State fund for fundamental researches of Ukraine within the Project Ф53.2/041.

[1] T. Valla, P.D. Johnson, Z. Yusof et al., Nature, 417(6889), 627 (2002).
[2] H. Kempa, P. Esquinazi, Y. Kopelevich, Phys. Rev. B. 65(24), 241101 (2005).
[3] N. Garcia, P. Esquinazi, J. Barzola-Quiquia et al. New J. Phys. 14, 053015 (2012).
[4] Y. Kopelevich, J.H. Torres, R.R. da Silva et al., Phys. Rev. Lett. 90(15), 156402 (2003).
[5] Y. Kopelevich, J.C. Medina Pantoja, R.R. da Silva et al., Phys. Rev. B 73(16), 165128 (2006).
[6] M. A. Howson, J. Phys. F: Met. Phys. 14, L25 (1984).
[7] V.F. Gantmacher, Electrons and Disorder in Solids (Clarendon, Oxford, 2005).
[8] E. McCann, K. Kechedzhi, Vladimir I. Fal'ko et al., Phys. Rev. Lett. 97(14), 146805 (2006).
[9] M.I. Zakharenko, T.V. Kalnysh, M.P. Semen`ko, Phys. Met. Metallogr. 113(8), 762 (2012).
[10] N.W. Ashcroft, N.D. Mermin, Solid State Physics (Holt, Rinehart and Winston, New York, 1976).
[11] C. Z. Wang, K. M. Ho, Phys. Rev. Lett. 71(8), 1184 (1993).

М.П. Семенько, М.І. Захаренко, Т.В. Калниш

Транспортні властивості нанокомпозитів графіт-метал

Київський національний університет імені Тараса Шевченка, фізичний факультет, вул. Володимирська, 64, 01601, МСП, Київ, Україна

Досліджено температурну поведінку електроопору терморозширеного графіту (ТРГ) і кобальтовмісних нанокомпозитів на його основі. Показано, що електричні властивості цих матеріалів можуть бути легко пояснені в рамках моделі слабкої локалізації. Також проаналізовано вплив металічного модифікатора на електротранспорт.

Ключові слова: терморозширений графіт, кобальт, електроопір, слабка локалізація; нанокомпозит.